

Cite this article as: Rare Metal Materials and Engineering, 2018, 47(8): 2290-2297.

ARTICLE

# Microstructure and Mechanical Properties of Transient Liquid Phase Bonded Joints of CB2 Ferritic Heat Resistant Steels with Amorphous BNi-2 Interlayer

He Hongjie, Sheng Guangmin, Liu Mingcan, Jiao Yingjun

Chongqing University, Chongqing 400044, China

**Abstract:** Microstructure and mechanical properties of transient liquid phase (TLP) bonded joints and the post bonding heat treatment (PBHT) for CB2 heat resistant steel using BNi-2 insert alloy were investigated. The Cr-rich borides and Cr-Mo borides generated in the transition region (TZ) and diffusion-affected zone (DAZ) reach the peak values in size and quantity when the isothermal solidification is completed. Subsequent elevation in bonding temperature and increment in bonding time result in gradual disappearance of such Cr-rich and Cr-Mo borides, as well as increased percent of BN precipitates. After PBHT the Cr-rich borides almost disappear while the size and amount of BN precipitates rise. The maximum tensile strength reaches to 934 MPa for the joint bonded at 1150 °C for 1800 s with elongation of only 5.3%. PBHT result in significant improvement in ductility of the joint as elongation of 20% is achieved with a decreased strength of 720 MPa, while the fracture takes place at base materials.

**Key words:** CB2 ferritic heat resistant steel; transient liquid phase (TLP) bonding; post bonding heat treatment (PBHT); Cr-rich boride; BN precipitate

CB2 ferritic heat resistant steels, a kind of high-temperature structural material, can be used in casings and valves for 620 °C ultra-supercritical power plants due to their high creep strength at elevated temperature and oxidation resistance<sup>[1]</sup>. However, premature failure is difficult to avoid at welded joints of CB2 steels and failure occurs in the heat-affected zone (HAZ) of the welds, due to the Type IV cracking in the fine grain region (FGHAZ). The reliable joining of CB2 steels is difficult with conventional fusion welding.

Transient liquid phase (TLP) bonding was developed by Duvall et al, and the composition and structure in TLP joints is homogenized, so the mechanical properties of TLP joints can reach or even exceed those of the base metals (BM)<sup>[2-4]</sup>. Existing literature reveals that the TLP can be successfully used to join Ni-based alloys<sup>[5,6]</sup>, stainless steels (SS)<sup>[7,8]</sup> and duplex stainless steels<sup>[9-12]</sup>. Recently, the amorphous BNi-2 insert alloy has been used to join the duplex SS<sup>[10]</sup>. Arafain investigated the TLP bonding of SS 410 and SS 321 using

BNi-2 interlayer<sup>[7]</sup>. Results revealed that, the predicted isothermal solidification time for the SS 321/BNi-2 combinations, by both migrating solid/liquid interface and solute distribution models, were in obvious disagreement with the SS 410/BNi-2 combinations owing to the presence of significant amount of Ni and Cr in the BM composition, and the diversity of composition can lead to various bonding reactions. Meanwhile, the TLP bonding of T91 steel using BNi-2 amorphous foil resulted in a bonding region stabilized by the high Ni concentration<sup>[13]</sup>. The micro-structural evolution and bonding behaviour of CB2 during TLP bonding have the discrepancy to T91. The study of the nickel based superalloy TLP bonded joints indicates that a proper PBHT has been previously proved to be feasible to eliminate the boride precipitates in diffusion-affected zone (DAZ), improving the degree of homogenization across bonding region<sup>[14-16]</sup>. However, the study of TLP bonding of CB2 and PBHT is rare and under development.

Received date: August 14, 2017

Foundation item: National Natural Science Foundation of China (51205428)

Corresponding author: Sheng Guangmin, Ph. D., Professor, College of Material Science and Engineering, Chongqing University, Chongqing 400044, P. R. China, Tel: 0086-23-65111826, E-mail: gmsheng@cqu.edu.cn

Copyright © 2018, Northwest Institute for Nonferrous Metal Research. Published by Elsevier BV. All rights reserved.

The present study is attempted to identify the microstructural evolution during bonding process and PBHT of CB2 and elucidate the correlation between the microstructure and mechanical property of the resulting joints.

## 1 Experiment

The chemical composition of the CB2 and BNi-2 in mass fraction is given in Table 1. Commercial BNi-2 amorphous foil with a thickness of 30  $\mu\text{m}$  and melting-temperature ranging from 970  $^{\circ}\text{C}$  to 1020  $^{\circ}\text{C}$  was selected as interlayer. CB2 was cut into 14 mm  $\times$  14 mm  $\times$  7 mm sub-sized specimens and the bonding surface of base alloys were ground up to 5000 grade by silicon carbide papers; base alloys and insert alloy were both ultrasonically cleaned with acetone. BNi-2 interlayer was then placed between the two base alloys during bonding process. TLP bonding was carried out in a furnace whose heating rate to the brazing temperature is 10  $^{\circ}\text{C}/\text{min}$  under a vacuum of  $1 \times 10^{-4}$  Pa. After TLP bonding and PBHT, the interfacial microstructure of joint was investigated by scanning electron microscopy (TESCA VEGAIII and JEOL JSM-7800F) equipped with energy dispersive spectrometer (EDS). The tensile test was conducted at room temperature using a universal testing machine with a travel speed of 1  $\text{m}/\text{min}$ .

## 2 Results and Discussion

### 2.1 Microstructure characteristics of joints

Fig.1 illustrates the microstructure of the joint prepared at 1050  $^{\circ}\text{C}$  for 60 s. The cross-section of the joint is divided into 3 distinct zones: isothermal solidification zone (ISZ), transition region (TZ), and diffusion-affected zone (DAZ). Fe is found to be absent in the interlayer, indicating the significant interdiffusion occurs between the filler and base material in Fig.2. In addition, the concentration profile of Ni exhibits a

decreasing tendency from the joint center toward the substrate. The considerable amount of Cr-rich borides is identified in the center region of the joint based on Fig.2 and Table 2, which indicates that this bonding condition is insufficient to complete the isothermal solidification<sup>[16]</sup>. The ISZ is a result of isothermal solidification including  $\gamma$ (Fe, Ni) and Cr-rich borides. The BN precipitates and Cr-rich borides present in the bonding interface and TZ. Zone C located in the DAZ

Table 1 Chemical composition of the materials (wt%)

	Fe	Ni	Cr	Si	B	Mo	Co	N
CB2	Bal.	0.3	9.4	0.2	0.008	1.5	1	0.02
BNi-2	3.5	Bal	7.0	4.4	2.75	-	0.003	-

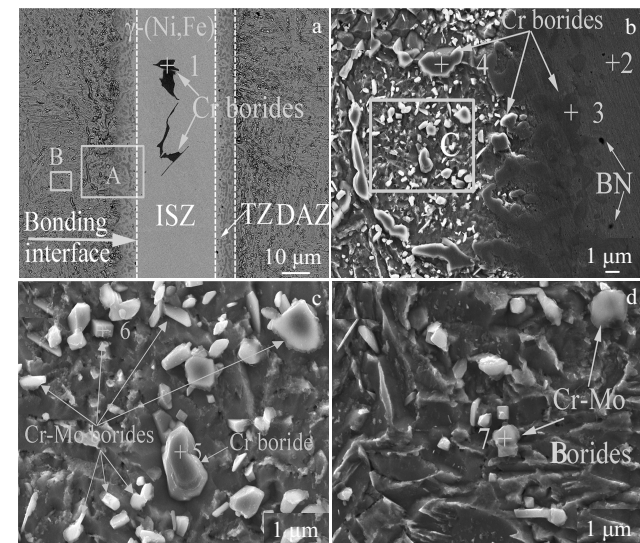


Fig.1 Microstructures of the joint prepared at 1050  $^{\circ}\text{C}$  for 60 s:  
(a) overview; amplification of zone A in Fig.1a (b), zone C in Fig.1b (c), and zone B in Fig.1a (d)

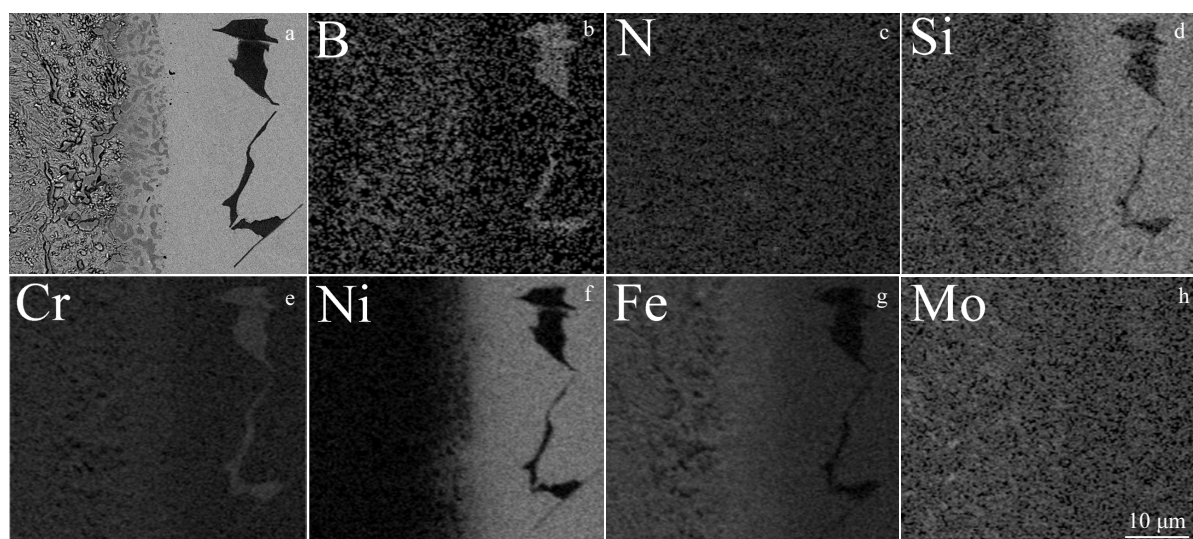


Fig.2 EDS analysis region (a) and element distributions (b-h) of the joint bonded at 1050  $^{\circ}\text{C}$  for 60 s

**Table 2** EDS analysis of marked points 1~7 for the TLP joint bonded at 1050 °C for 60 s in Fig.1 (wt%)

Point	Fe	Ni	Cr	Si	B	Mo	Possible Phase
1	3.1	9.73	56.0	0.81	28.9	0.93	Cr-rich boride
2	54.9	32.6	8.4	1.58		0.96	$\gamma$ -(Ni, Fe)
3	71.1	8.92	16.9	0.27		1.01	Cr boride
4	74.2	0.38	21.8	0.08		1.38	Cr boride
5	70.2	0.87	24.3	0.12		2.23	Cr boride
6	68.6	0.94	16.3	0.41		12.2	Cr-Mo boride
7	62.8	0.84	18.8	0.24		15.4	Cr-Mo boride

includes the Cr-rich borides distribution in the grain boundary and the smaller Cr-Mo borides within grain. The maximum solubility of Si in  $\gamma$ -Fe and Ni are 3.8 wt% and 10 wt%, respectively. The radius of the Si (110 pm) is larger than that of B (80 pm), so Si is hard to go through the interface of interlayer and substrate; as a result the Si is mainly distributed in ISZ, and the small quantity of Si in DAZ is not precipitated with Cr.

Fig.3 and Fig.4 show the microstructures of the CB2 TLP bonding joints. The width of the ISZ increases significantly as the bonding condition extent changes from 1050 °C for 60 s to 1150 °C for 7200 s. The Cr-rich borides in the central bonding region disappear as the temperature reaches to 1100 °C. The number of Cr-rich borides in TZ and DAZ reaches the maximum value when the isothermal solidification is about to complete in Fig.3b. The bonding temperature (1150 °C) is still lower than the borides solvus temperature, but the number of

Cr-rich borides and Cr-Mo borides in the joints is found to decline. The reasons are because the solubility of B in the BM is raised and the content distribution of B in the BM becomes more uniform with the increasing of bonding time and temperature [9,17].

## 2.2 Mechanical properties

Fig.5a shows the stress-strain curves of the joints at 1050, 1100 and 1150 °C for 60 s. Fig.5b depicts the tensile strength of the joints at 1150 °C for 1800, 3600, and 7200 s. The maximum tensile strength of 934 MPa is obtained when the bonding time extends to 1800 s.

## 2.3 Fracture morphology observation

The fracture surface of the joint bonded at 1050 °C for 60 s contains two regions, as shown in Fig.6. The particles in the  $\gamma$ -(Ni, Fe) dimples (region B) are recognized as BN precipitates based on Fig.6c and Fig.7a, Cr-rich borides occur in fracture surface based on Fig.6b and Fig.7a, while region A and B may correspond to the bonding interface. Fig.8a and 8b show the similar failure morphology of the joints bonded at 1100 and 1150 °C for 60 s which both embody two regions. As shown in Fig.8c and 8d, the most significant change is that the BN precipitates are detected both in region A and B comparing with Fig.6. The ductile fracture surfaces of the joints bonded at 1150 °C for 1800 and 3600 s have the uniform morphology both including 3 regions in Fig.9, region A and B are the same kind of failure morphology, the mainly phases of the surface are BN and  $\gamma$ -(Ni, Fe) based on Fig.7c. The percent of the BN

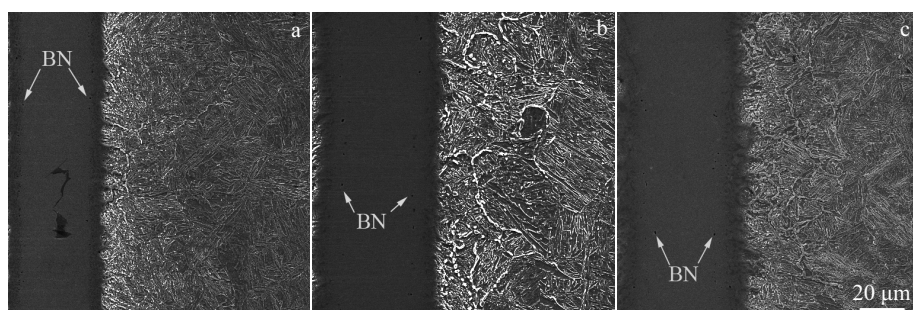


Fig.3 Microstructures of the joints prepared at 1050 °C (a), 1100 °C (b), and 1150 °C (c) for 60 s

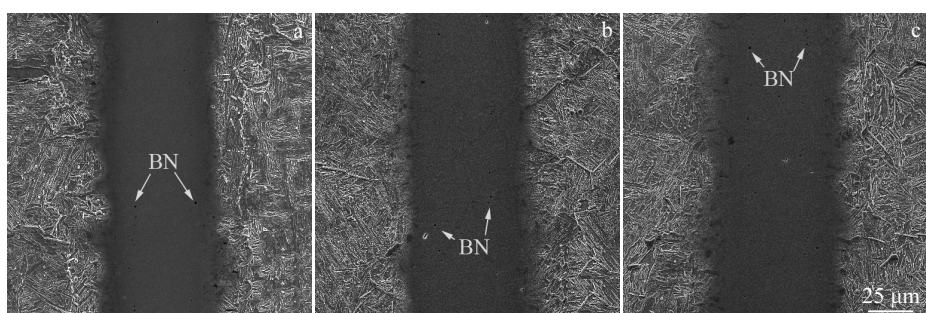


Fig.4 Microstructures of the joints prepared at 1150 °C for 1800 s (a), 3600 s (b), and 7200 s (c)

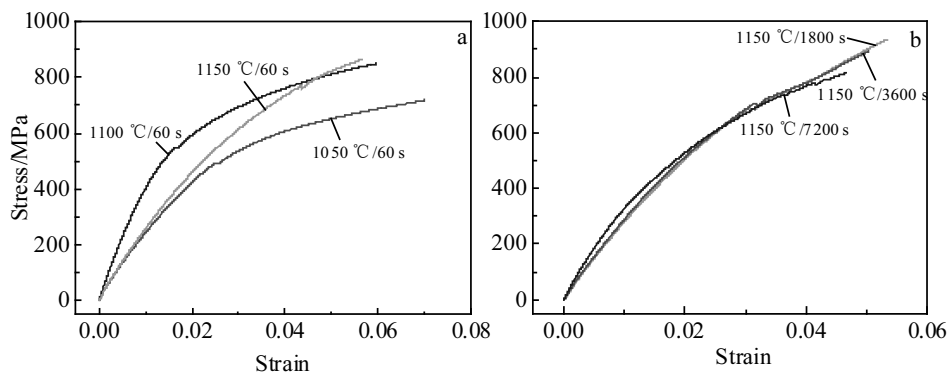


Fig.5 Stress-strain curves of the joints at 1050, 1100 and 1150 °C for 60 s (a) and at 1150 °C for 1800, 3600, and 7200 s at (b)

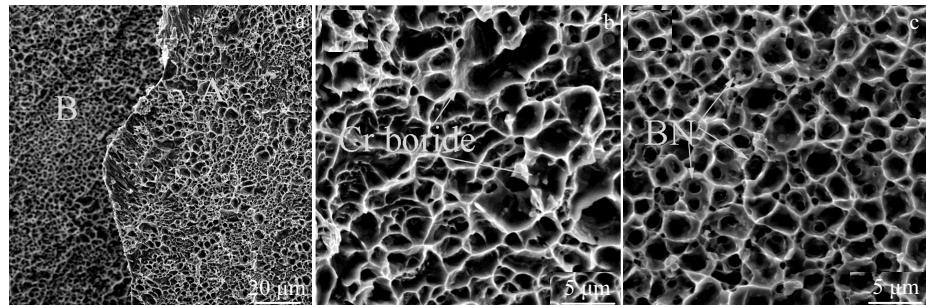


Fig.6 Fracture surface morphologies of the joints bonded at 1050 °C for 60 s: (a) overview; amplification of region A (b) and region B (c) in Fig.6

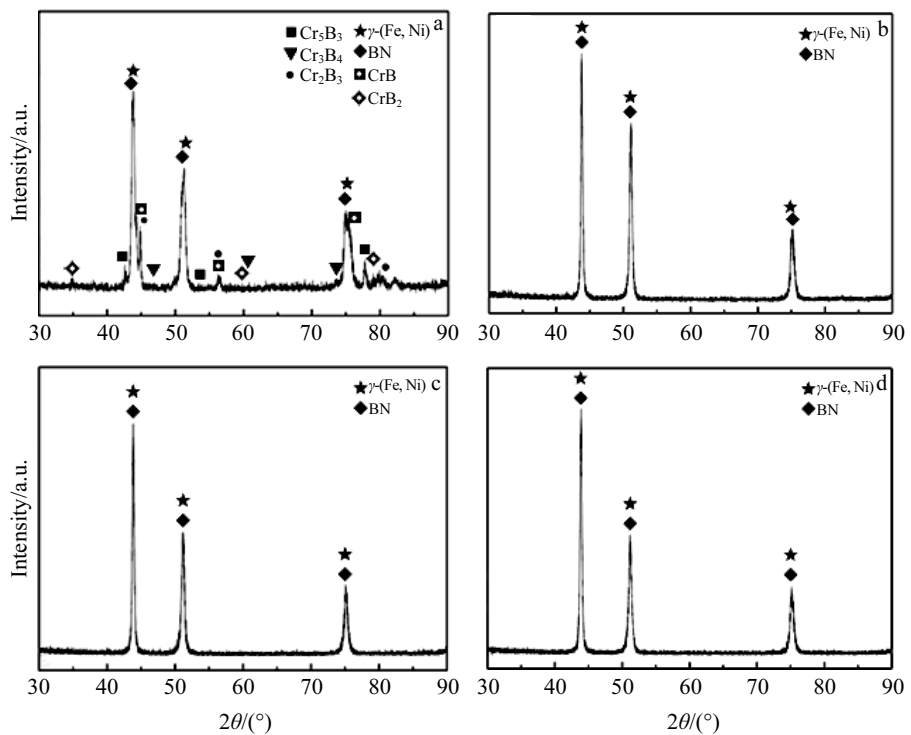


Fig.7 XRD patterns of fracture surface after tensile testing of joints: (a) 1050 °C for 60 s, (b) 1150 °C for 60 s, (c) 1150 °C for 1800 s, and (d) 1150 °C for 7200 s

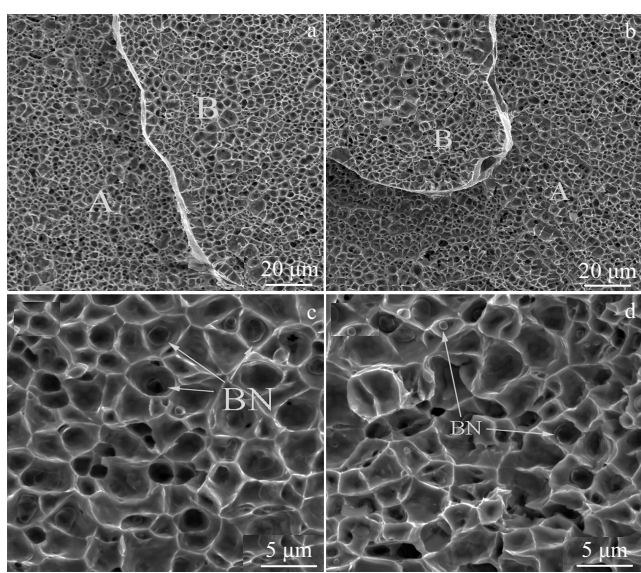


Fig.8 Fracture surface morphologies of the joints bonded with BNi-2 at 1100 °C for 60 s (a), at 1150 °C for 60 s (b); amplification of region A (c) and region B (d) in Fig.8b

precipitates and size of the scattered BN particles in the fracture surface in Fig.9d and 9e both are elevated as the bonding time increased. The secondary precipitates in Fig. 9f are the precipitated BN phase. The fracture surface of the joint bonded at 1150 °C for 7200 s includes 3 zones in Fig.10. The sizes of BN precipitates located in region A and B both are enhanced, and there are many smaller BN particles in large scale  $\gamma$ -(Ni, Fe)

grains in region C according to Fig. 10 and Fig. 7d.

The failure process of the CB2 joints are concluded to be 2 main actions. One is that ductile fractures take place through the bonding interface, and the other one is that fractures present in ISZ where BN perceptions occur. The tensile strength of the joint is affected by the strength of bonding interface and ISZ, Cr boride and BN precipitate. The strength of bonding interface and ISZ are enhanced with the increase of bonding temperatures and time, since higher bonding temperature and time can boost interdiffusion of BM and insert layer, and the uniform distribution of elements and the reduction in segregation of alloying elements are beneficial to the joint strength simultaneously<sup>[9]</sup>. The distribution evolutions of Cr borides are summarized as three stages. First, a number of tiny Cr borides lie in TZ at 1050 °C for 60 s. Second, the number of Cr-rich borides in the TZ begins to decrease, and the reticular precipitates present in the DAZ. Last, the Cr borides disappear both in the TZ and DAZ with the further increase of temperature and time. It is worth noting that the distance of the BN particles distributed in two sides of bonding central the line have same value which approximately equals to the thickness of BNi-2 interlayer, about 30 μm according to Fig.3 and Fig.4. The brittle BN precipitates are not removed after formed in the interface of insert alloy and CB2. B and N meet each other on the interface during TLP process, N is a strong boride forming element and BN is more stable than other borides that indicate the formation of BN is of priority<sup>[9,18]</sup>. It is hard to detect the BN particles in the TZ and DAZ, and the N roots in BM can promote the growth of BN particles in the interface.

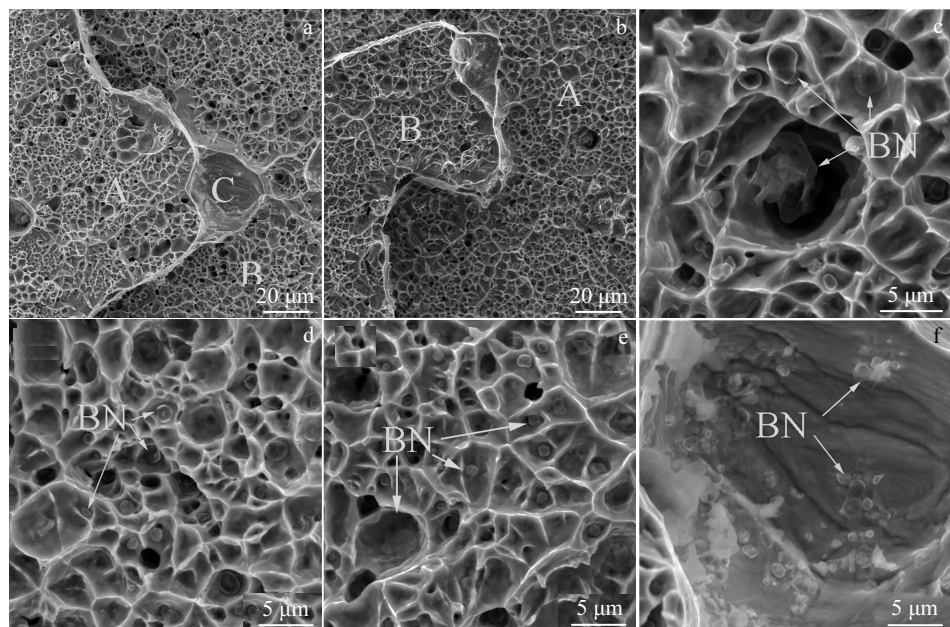


Fig.9 Fracture surface morphologies of the joints bonded with BNi-2 at 1150 °C: (a) overview for 1800 s, (b) overview for 3600 s; amplification of region A in Fig.9b (c), region B (d), region A (e), and region C in Fig.9a (f)

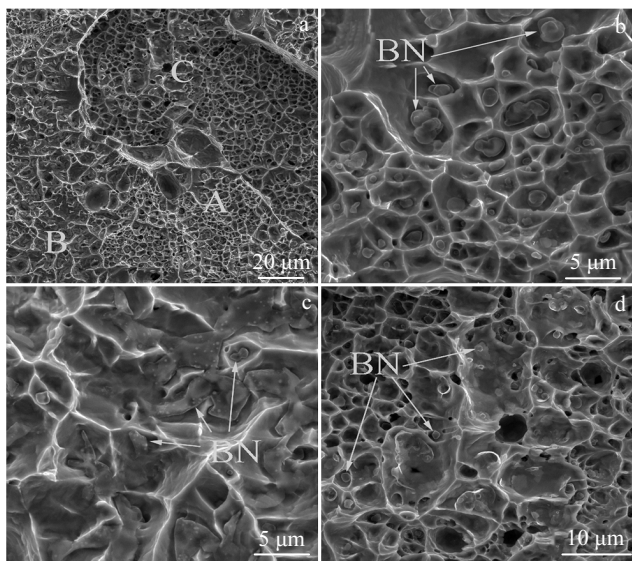


Fig.10 Fracture surface morphologies of the joints bonded with BNi-2 at 1150 °C for 7200 s: (a) overview; amplification of region A (b), and region B (c), and region C in Fig.10a (d)

The Cr-rich borides and BN precipitates could partially create inhomogeneous deformation, because the dislocation piling up in the grain boundaries and interface between matrix and brittle particles can lead to high local stress concentration during deformation<sup>[19]</sup>. Thus, the borides become the preferential position to crack and reduce the tensile strength of the joint<sup>[6,19]</sup>. The fracture of the joint bonded at 1050 °C for 60 s takes place at the bonding interface with a lower tensile strength owing to the Cr-rich borides and BN precipitates distributed in the area. The tensile strength of the joints bonded at 1100 and 1150 °C for 60 s have an obvious improvement, because the strength of bonding interface and ISZ increases, and Cr-rich borides almost disappear. The joint bonded at 1150 °C for 1800 s possesses the highest tensile strength due to the increased strength of bonding interface and ISZ and the unobvious change of BN sizes. The tensile strength of the joint has a significant decrease as a result of the increased percent of BN precipitates in ISZ, big size of BN particles and  $\gamma$ -(Ni,Fe) in the fracture surface in Fig.10. The elongation of the TLP joints are much lower than that of the raw BM due to the formation of borides during TLP bonding<sup>[5,19]</sup>.

#### 2.4 Post bonding heat treatment

In PBHT procedure, joints bonded at 1050, 1100 °C for 60 s, and 1150 °C for 1800, 3600 s were investigated. PBHT of 1100 °C/1.5 h AC + 750 °C/8 h AC (AC: air cooling) was applied. It is obvious that the Cr-rich borides in DAZ and TZ nearly disappear.

The effect of the Cr-rich borides on the tensile strength can be neglected, as shown in Fig.11. The tensile strength of the PBHT joint mainly depends on the strength of ISZ and

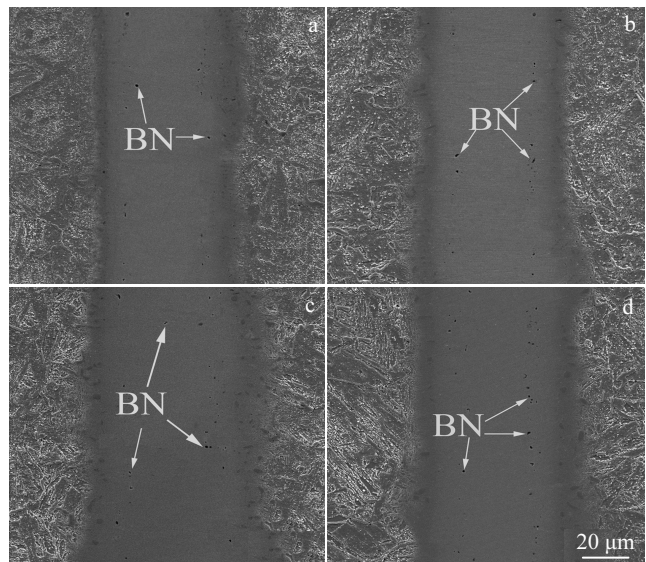


Fig.11 Microstructures of the PBHT joints prepared using BNi-2 at 1050 °C for 60 s (a), 1100 °C for 60 s (b), 1150 °C for 1800 s (c), and 1150 °C for 3600 s (d)

bonding interface, BN precipitates. The widths of ISZ show an obvious increasing trend after PBHT, which indicates that the degree of homogenization across bonding regions is improved, which is beneficial to mechanical properties of the joints. And the boundaries of the bonding interface become more blurred after PBHT; long-time diffusion can increase the joint strength effectively<sup>[17]</sup>. The percent of BN in the fracture surface of the PBHT joints significantly increases against to the joints before PBHT, but there is no obvious distinction between fracture surfaces of the PBHT joints bonded at 1050 and 1100 °C for 60 s. Meanwhile, the percent of BN precipitates of the joints has no evident variety in Fig.11. The phenomenon can explain why B in bonding region becomes more homogeneous, and the content of N in bonding region is limited. The increasing percent of BN precipitate in ISZ is negative to the tensile strength. The fractures of PBHT joints

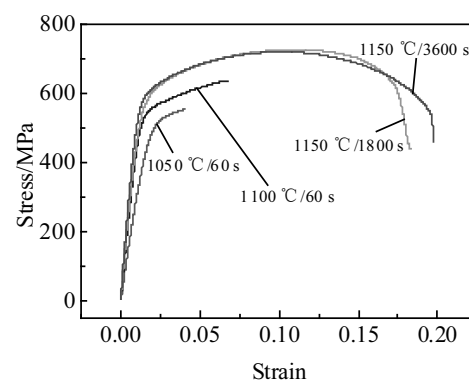


Fig.12 Stress-strain curves of the joints bonded with BNi-2 after PBHT

bonded at 1050 and 1100 °C for 60 s take place through the ISZ with low tensile strength, as shown in Fig.12 and Fig.13, which is attributed to the increasing percent of BN particles. The PBHT joints at 1150 °C for 1800 and 3600 s acquire a lower tensile strength with a typical ductile fracture, which

better coincides with the raw CB2 (690 MPa), and a fine extensibility (0.2) is acquired with the raw CB2 (0.15) displayed in Fig.12 and Fig.14. The tensile strength of BM after bonding at 1150 °C for 1800 s is 934 MPa which is higher than that of the raw BM, owing to the raised amount of

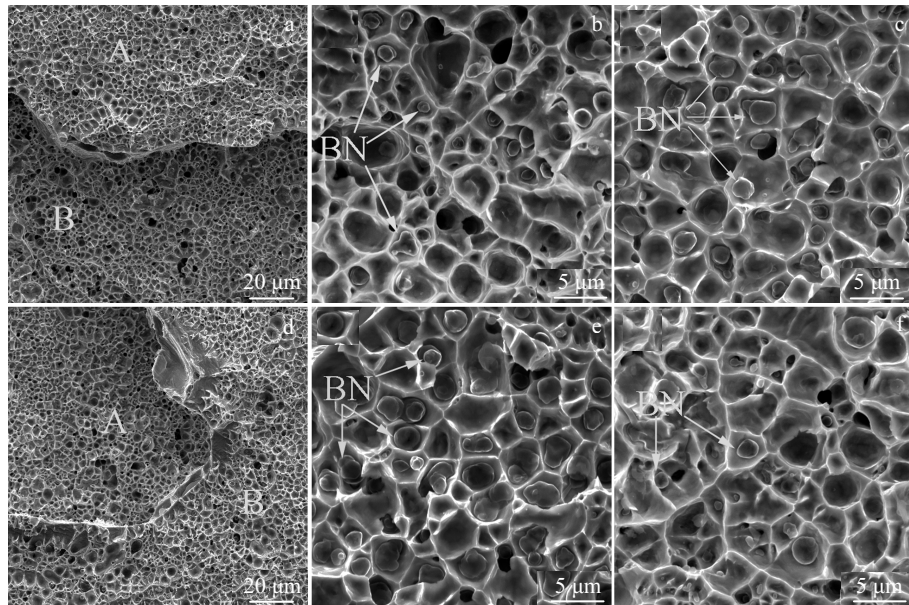


Fig.13 Fracture surface morphologies of the joints bonded with BNi-2 after PBHT: (a) at 1050 °C for 60 s and amplification of region A (b) and region B (c) in Fig.13a; (d) at 1100 °C for 60 s and amplification of region A (e) and region B (f) in Fig.13d

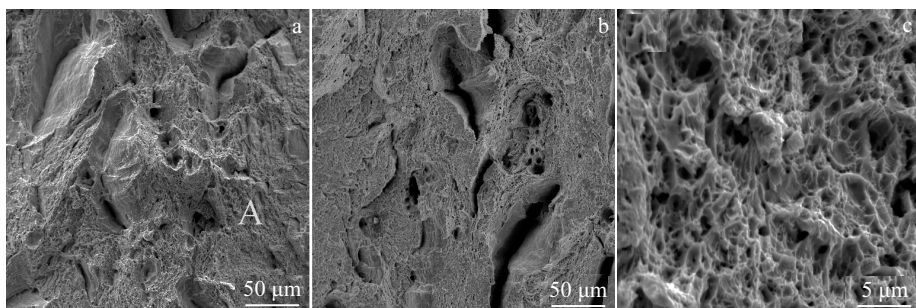


Fig.14 Fracture surface morphologies of the joints bonded with BNi-2 after PBHT at 1150 °C for 1800 s (a), 3600 s (b), and the amplification of region A in Fig.14a (c)

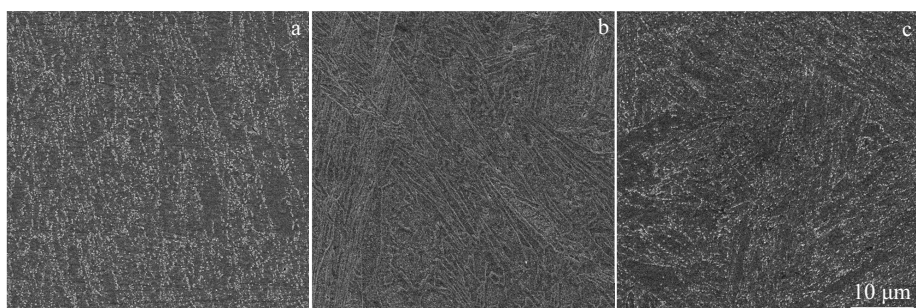


Fig.15 Microstructures of the base materials: (a) raw CB2, (b) bonded at 1150 °C for 1800 s, and (c) after PBHT

the martensite lath after bonding in Fig.15b. The BM after PBHT gets similar microstructure to the raw BM, as shown in Fig.15. It is concluded that the mechanical property of TLP-bonded joints is optimized through PBHT technique.

### 3 Conclusions

1) Cr-rich borides occur in the central bonding region during the isothermal solidification, and disappear after isothermal solidification completed.

2) The Cr-rich borides are found in the TZ and DAZ. The percent of Cr-rich boride rises to the peak value at 1050 °C for 60 s in TZ, and reaches to the maximum at 1100 °C for 60 s in DAZ. The Cr-rich boride precipitates in TZ and DAZ gradually disappear with the increase of bonding temperature and time. BN precipitates are retained at the original interlayer/CB2 interface which have a negative effect on mechanical properties. And the percent of BN precipitates in ISZ is enhanced as the bonding temperature and time increase.

3) Tensile strength of the joint reaches to the maximum of 934 MPa at 1150 °C for 1800 s while elongation is only 5.3%.

4) Cr-rich borides almost disappear while the percent of BN particles in fracture surface increases obviously after PBHT. The tensile strength of joints bonded at 1150 °C for 1800 and 3600 s match that of the raw CB2 720 MPa, with a considerably improved elongation of 20% after PBHT when the fracture takes place at BM.

### References

- 1 Výrostková A, Falat L, Kepič J et al. *Metal*[J], 2010
- 2 Aluru R, Gale W F, Chitti S V et al. *Materials Science and Technology*[J], 2008, 24(5): 517
- 3 Kim D U, Nishimoto K. *Materials Science and Technology*[J], 2003, 19(4): 456
- 4 Liu Jide, Jin Tao, Zhao Nairen et al. *Rare Metal Materials and Engineering*[J], 2007, 36(2): 332 (in Chinese)
- 5 Mosallaee M, Ekrami A, Ohsasa K et al. *Metallurgical and Materials Transactions A*[J], 2008, 39(10): 2389
- 6 Zhang L X, Sun Z, Xue Q et al. *Materials & Design*[J], 2016, 90: 949
- 7 Arafin M A, Medraj M, Turner D P et al. *Materials Chemistry and Physics*[J], 2007, 106(1): 109
- 8 Hong L, Zhuoxin L, Yingling W et al. *Rare Metal Materials and Engineering*[J], 2011, 40(8): 1382 (in Chinese)
- 9 Yuan X, Kim M B, Cho Y H et al. *Metallurgical and Materials Transactions A*[J], 2012, 43(6): 1989
- 10 Yuan X, Kim M B, Kang C Y. *Metallurgical and Materials Transactions A*[J], 2011, 42(5): 1310
- 11 Yuan X, Kim M B, Kang C Y. *Materials Characterization*[J], 2009, 60(11): 1289
- 12 Padron T, Khan T I, Kabir M J. *Materials Science and Engineering A*[J], 2004, 385(1): 220
- 13 Chen S J, Tang H J, Jing X T. *Materials Science and Engineering A*[J], 2009, 499(1): 114
- 14 Pouranvari M, Ekrami A, Kokabi A H. *Materials Science and Engineering A*[J], 2013, 568: 76
- 15 Pouranvari M, Ekrami A, Kokabi A H. *Journal of Alloys and Compounds*[J], 2009, 469(1): 270
- 16 Cao J, Wang Y F, Song X G et al. *Materials Science and Engineering A*[J], 2014, 590: 1
- 17 Chen B, Xiong H P, Mao W et al. *Welding in the World*[J], 2015, 59(6): 911
- 18 Abe F. *Procedia Engineering*[J], 2011, 10: 94
- 19 Yang Y H, Xie Y J, Wang M S et al. *Materials & Design*[J], 2013, 51: 141

## 以 BNi-2 非晶为中间层的 CB2 耐热钢瞬时液相扩散连接的接头组织和性能研究

何洪杰, 盛光敏, 刘铭灿, 焦英俊

(重庆大学, 重庆 400044)

**摘要:** 主要研究采用 BNi-2 非晶态中间层的 CB2 耐热钢瞬时液相 (TLP) 扩散连接接头组织和性能, 及焊后热处理 (PBHT) 对接头组织和性能的影响。富 Cr 硼化物 和 Cr-Mo 硼化物出现在接头的过渡区和扩散影响区, 其尺寸和数量在等温凝固完成时达到最大值。随着连接温度和时间的增加, 富 Cr 的硼化物和 Cr-Mo 硼化物逐渐减少, 而 BN 相逐渐增多。经过焊后热处理后, 接头的富 Cr 硼化物几乎全部消失, 而 BN 相的尺寸和数量增加。在热处理之前, 焊接温度为 1150 °C, 保温时间 1800 s 的接头有最大抗拉伸强度, 为 934 MPa, 延伸率为 5.3%。通过焊后热处理, 断裂发生在母材, 而其延伸率显著提高到 20%, 而抗拉伸强度降低到 720 MPa, 其性能与原始的母材性能相近。

**关键词:** CB2 耐热钢; 瞬时液相焊接; 焊后热处理; 富 Cr 硼化物; BN 相

作者简介: 何洪杰, 男, 1992 年生, 硕士, 重庆大学材料科学与工程学院, 重庆 400044, 电话: 023-65111826, E-mail: cervus24@163.com